MEDWIN PUBLISHERS
Committed to Create Value for Researchers

Open Access Journal of Pharmaceutical Research
ISSN: 2574-7797

Facile Synthesis of Copper Sulphide Nanoparticles using Trichoderma Harzianum and Antibacterial Efficiency Enhancement by Gentamicin Sulfate

Abishad P[1,2,3], Namratha K[4], Nayan MB[1], Jayashankar M[3], Srinath BS[3], Jess V[4] and Byrappa K[1,5]*

[1]Center for Material Science and Technology, University of Mysore, India

[2]Department of Veterinary Public Health, College of Veterinary and Animal Sciences, Kerala Veterinary and Animal Sciences University, India

[3]Department of Studies and Research in Microbiology, Mangalore University, India

[4]Department of Studies in Earth Science, Centre for Advanced Studies in Precambrian Geology, University of Mysore, India

[5]Center for Research and Innovations, BGSIT, Adichunchanagiri University, India

Research Article

Volume 6 Issue 2

Received Date: March 31, 2022

Published Date: June 20, 2022

DOI: 10.23880/oajpr-16000268

***Corresponding author:** Byrappa K, Centre for Research and Innovations, BGSIT, Adichunchanagiri University, B.G. Mandya-571 418, India; Email: kbyrappa@gmail.com

Abstract

The application of biosynthesized semiconductor nanomaterials has gained recent attention towards pathogenic bacteria. This study reports cost- effective, eco- friendly biosynthesis of copper sulphide nanoparticles (CuS NPs) employing the fungal cell mass of the biocontrol pest, T. harzianum. Later, gentamicin was loaded onto the mycosynthesised CuS NPs to assess the enhancement in its antibacterial activity. A synergistic antibacterial efficacy was observed for the GS- laden CuS NPs against the pathogens tested (E. coli, Salmonella Typhi, Klebsiella pneumoniae, Staphylococcus aureus and Bacillus subtilis). The green synthesized CuS NPs as well as GS- laden CuS NPs were found to be relatively non- toxic towards MDA MB- 231 epithelial cell line. In short, the GS- laden CuS NPs were found to be an effective candidate to combat pathogenic microorganisms. The present study highlights the facile synthesis of semiconductor nanomaterials which could act as potential drug carrier and opens the feasibility of biocompatible materials for drug loading in the field of nanomedicine.

Keywords: Copper Sulphide; Gentamicin sulfate; Mycosynthesis; Nanoparticle; Trichoderma harzianum

Abbreviations: CuS NPs: Copper Sulphide Nanoparticles; GS: Gentamicin Sulfate; PD: Potato Dextrose; FTIR: Fourier Transform Infra-Red Spectroscopy; DLS: Dynamic Light Scattering; TGA: Thermo Gravimetric Analysis; DTA: Differential Thermal Analysis; PXRD: Powder X-Ray Diffraction; AFM: Atomic Force Microscopy; SEM: Scanning Electron Microscopy; BCA: Bicinchoninic Acid; LC: Loading Capacity; EE: Entrapment Efficiency; AMR: Antimicrobial Resistance; SPR: Surface Plasmon Resonance; EDX: Energy Dispersive X-Ray; NP: Nanoparticles.

Introduction

Gentamicin belongs to the aminoglycoside group of antibiotics which is commonly employed to treat a variety of bacterial infections of the bone, meninges, urinary tract, as well as the conditions like sepsis and pelvic inflammatory disease. Moreover, it is considered as a first- line aminoglycoside candidate to treat several pathogenic microbes such as Proteus vulgaris, Pseudomonas aeruginosa, Escherichia coli, Enterobacter aerogenes, Klebsiella pneumoniae, and Staphylococcus aureus [1]. Of late, antimicrobial resistance (AMR) has emerged as a global public health threat and is regarded as an evolutionary process that often arises due to the indiscriminate use of antibiotics in both human and veterinary practice. Generally, the misuse and overuse of antibiotics have led to the development of drug resistance among the bacterial pathogens, which results in a serious public health concern in terms of treating the infections of bacterial origin [2,3]. Additionally, the emergence of AMR has recently been associated widely due to the impaired efflux pumps and the genetic modification of suitable enzymes that would reduce the efficacy of antimicrobials against bacterial agents [4].

Generally, the antibiotics have a short half-life and the levels of antibiotic concentration at target sites may fluctuate. The desired concentration of antibiotic would be attained at the site of infection by practicing effective drug delivery systems. Nanotechnology- mediated delivery system offers a promising approach for restoring and enhancing the effectiveness of conventional antibiotics by providing the intra-cellular drug targeting and sustained release into the targeted cells [1]. The nanoparticle (NP)- based drug delivery systems could accelerate the bioavailability of antibiotics which would further enhance its therapeutic efficacy [5]. Moreover, such NP- based delivery systems can overcome the difficulties in frequent antibiotic dosing as well as fluctuating levels of antibiotics which would otherwise lead to a lowered therapeutic index [6]. Of late, hollow copper sulphide (CuS) NPs were widely employed as effective antibiotic delivery vehicles (~55 nm diameter) through transdermal drug delivery using thermal ablation [7]. The synthesis of CuS NPs can be achieved either by hydrothermal [8], solvothermal [9] or biological synthesis [10]. While the former techniques (hydrothermal as well as solvothermal) utilize the high temperature, pressure, and toxic chemicals such as hydrogen sulphide for the synthesis of CuS NPs, the latter (biological) could avoid the utility of such methods. Among the various methods for biological synthesis, mycosynthesis (fungi mediated) exhibits elevated metal bioaccumulation ability and tolerance that could be beneficial for the biosynthesis of CuS NPs [11].

Although the fungi mediated biosynthesis can be considered as an ideal approach for the synthesis of CuS NPs, the exact underlying antimicrobial mechanism of CuS NPs has not fully been revealed [12]. The fungal cells produce extracellular enzymes and secondary metabolites which could accelerate the biosynthesis of NPs [13]. The prepared CuS NPs were thus used to treat the bacterial infections by binding them to the 30S ribosomal subunit of the pathogens without damaging the host cells and in turn inhibiting the protein synthesis [14]. Moreover, the extracellular synthesis of CuS NPs was reported from the copper ore mine wastewater while employing the fungus Fusarium oxysporum for the removal of high load copper metal contaminants [1,15]. The present study was carried out with an objective to synthesis, characterize and evaluate the antibacterial potential of CuS NPs employing the fungal cell mass of Trichoderma harzianum (biocontrol pest). Further, gentamicin was loaded onto the green synthesized CuS NPs in order to assess the enhancement in its antibacterial activity.

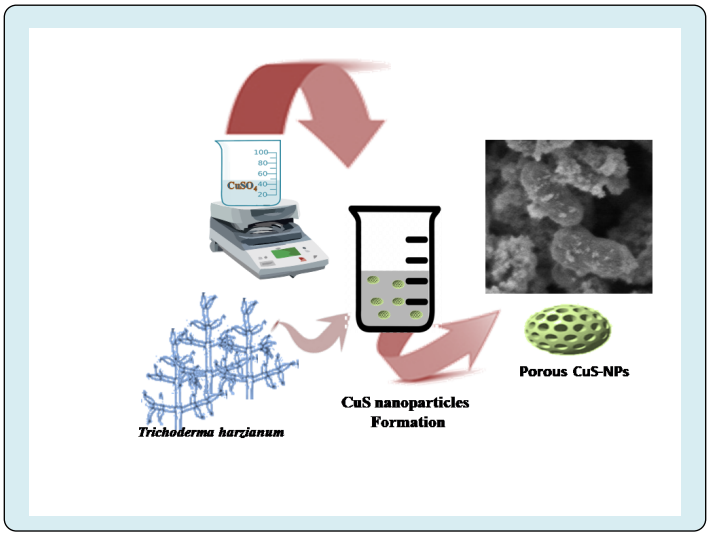

Materials and Methods

Microorganisms and Chemicals

The chemicals- CuSO4.3H2O (99.99%), gentamicin sulfate (GS), methanol and isopropanol (Fisher, UK), nutrient agar media, potato dextrose (PD) agar, RBC diluting buffer, glutaraldehyde (HiMedia, India) were used in the present work. The standard bacterial strains of S. aureus (MTCC 6908), Salmonella Typhi (MTCC 733), K. pneumoniae (MTCC 661), Bacillus subtilis (MTCC 121) and E. coli (MTCC 1698) were procured from the Microbial Type Culture Collection Center and Gene Bank, IMTECH, Chandigarh, India.

The fungal culture of T. harzianum obtained from the Kerala Agricultural University, India was employed in this study for the biosynthesis of CuS NPs. An initial concentration of the fungal culture (0.15 mg/mL) inoculated onto the PD agar medium was incubated at 25 to 28°C for 6 days to observe the formation of emergent mycelia. The morphological characteristics and microscopic examination were carried out to confirm the fungal culture.

Mycosynthesis of CuS NPs

The fungal cultures of T. harzianum grown in Erlenmeyer flasks containing PD broth media (150 mL) were incubated at 25 to 28°C under shaking conditions (200 rpm) for 6 days were used for the experiment. Subsequent to the culturing, the fungal mycelia were removed from the media by centrifugation (6000 rpm for 10 min at 5°C); the settled mycelia were washed twice in sterile nanopure water. Later, the harvested fungal cell mass (5 g) was dispersed in sterile nanopure water (50 ml) kept in Erlenmeyer flasks at pH 5.0-6.0. To this suspension, aqueous solution of copper sulphate at various concentrations (1 mM, 2 mM, 5 mM and 10 mM) were added and kept on a shaker for 180 rpm at 25°C and the synthesis of CuS NPs was carried out for a period of 36 h.

Characterization of CuS NPs

The CuS NPs obtained were further characterized by UV-Vis spectroscopy, Fourier transform infra- red spectroscopy (FTIR), dynamic light scattering (DLS), Thermogravimetric analysis (TGA) and differential thermal analysis (DTA), powder X-ray diffraction (PXRD), atomic force microscopy (AFM) as well as scanning electron microscopy (SEM).

In order to determine the UV- Vis spectroscopic analysis, the obtained CuS NPs were dissolved in ultrapure water (1 mg/ml) and scanned in the range of 350 to 650 nm (SA-165, Elico, India). Besides, the obtained CuS NPs were freeze dried to identify the unknown functional groups by using FTIR analysis (JASCO FTIR- 460 Plus Spectrophotometer, Japan) at room temperature in the range of 400- 4000 cm-1 along with potassium bromide wafers. The size distributions of the mycosynthesised CuS NPs were estimated by dynamic light scattering (BIC 90 Plus, Brookhaven Instruments Corp., USA) performed at an angle of 90o at 25°C. The TGA- DTA of CuS NPs were then carried out by heating around 18 mg of samples in nitrogen atmosphere at a rate of 30°C per min in the range of 50 to 900°C (NETZSCH STA 2500, Germany).

In order to assess the crystalline structure of the biosynthesized CuS NPs, PXRD analysis (Rigaku Smart Lab, Japan), was performed by CuKα radiation using 40 KeV and 30 mA with a scanning step size of 0.02°and λ=1.544Å. Additionally, the surface texture of biosynthesized CuS NPs was studied using AFM (APE Research, Italy). Further, the morphology of CuS NPs was evaluated by examining the samples using SEM (JEOL JSM-6610 LV, Japan).

In Vitro Cytotoxicity Assay

The effect of CuS NPs on the cell viability was estimated by in vitro MTT cytotoxicity assay [16]. Briefly, the MDA MB-231 epithelial cell lines (1 × 105 cells per ml; 100 µl per well) were seeded in a 96 well plate, with replicates. Later, the cells were treated with varying concentrations (0, 5, 10, 25, 50, 100 µg/ml) of CuS NPs for 24 and 48 h. Subsequent to the incubation, MTT stock solution (5 mg/ml; 20 µl) was added to each of the well and incubated at 37oC for 4 h. The formazan crystals thus obtained were solubilized with dimethyl sulfoxide (DMSO) and the absorbance was measured at 570 nm using a microplate reader (BioRad, USA) to determine the cell viability. The cell viability (expressed in %) was calculated as, cell viability= (Absorbance of treated cell / Absorbance of control cells) × 100.

SEM Imaging of CuS Treated Bacteria

The SEM imaging was performed to visualize the morphological changes of B. subtilis strains (taken as representative) treated with CuS NPs (80 µg/mL) for 60 min. The overnight fixed bacterial cells (2% glutaraldehyde) on clean grease- free glass coverslips were dehydrated (ethanol) and visualized for electron microscopy (JEOL JSM-6610 LV SEM, Japan).

Preparation of GS- Laden CuS NPs

The aminoglycoside antibiotic GS was loaded onto the mycosynthesised CuS-NPs. Briefly, CuS NPs (7 mg) was added to the nanopure water (10 ml) and the mixture was stirred mildly at 400 rpm for 5 min. Subsequently, GS (16 mg) added into this mixture was stirred at 1400 rpm for 2 h to form the GS loaded CuS NPs; the mixture was maintained for 5 min. Finally, the suspension was centrifuged (Eppendorf AG

5810R, Germany) at 12,000 rpm for 10 min to separate the nanoparticles.

In order to investigate the physical stability of lyophilized GS loaded CuS NPs, the optimized formulation was freeze-dried (Hawarch Scientific, China) in the presence of sucrose (0.10% w/v) as a cryoprotectant for 48 h at 0.05 mm Hg pressure. The freeze-dried samples stored at room temperature (at 25°C) were then redispersed by vortex mixing with 10 ml of ultra-pure water.

Drug Loading and Entrapment Efficiency

The amount of GS entrapped in the CuS NPs was determined as described earlier [17], with slight modifications. The GS loaded CuS NPs was centrifuged10000 rpm for 30 mins, and the supernatant was collected. The bicinchoninic acid (BCA) protein estimation assay was employed to determine the concentration of GS present in the supernatant, thus providing the mass of protein remaining unencapsulated. A mass balance was performed to determine the amount of GS that was loaded into the microspheres. The loading capacity (LC; in %) of GS on CuS NPs was calculated as (Entrapped drug /nanoparticle weight) × 100.

The protein that was lost while washing the microspheres during fabrication process could not be considered while calculating the LE; hence, the LE would slightly be overestimated. The entrapment efficiency (EE; in %) of the protein was therefore determined as [(drug added-free unentrapped drug)/nanoparticle weight] × 100.

In Vitro Haemolytic Assay

The in vitro haemolytic assay of GS loaded CuS NPs were performed in chicken RBCs [18]. Briefly, the freshly collected aseptic chicken blood was centrifuged at 3000 rpm for 5 min, and the erythrocyte pellet obtained was washed four times with sterile normal saline (0.85%) solution. Subsequent to the repeated washing, sterile PBS was added to the erythrocyte pellet so as to obtain 10% suspension of chicken RBCs. Later, the haemolytic activity of the GS loaded CuS NPs (100 µg/mL) was assessed by estimating the absorbance of supernatant at 543 nm (Beckman Coulter DU 730, USA), keeping Triton-X 100 (0.10%) as the positive control.

In Vitro Antibacterial Activity

In order to evaluate the synergistic effect of the antibiotic GS with the mycosynthesised CuS NPs, in vitro antibacterial assay was performed against both Gram- negative (K. pneumonia, S. Typhi and E. coli) as well as Gram-positive (S. aureus, and B. subtilis) bacteria in a well diffusion assay. The sterile pre- warmed Muller Hinton agar plates seeded with the test bacterial suspension (1 x 106 CFU) were treated with different concentrations of GS alone (30 µg), CuS NPs (80 µg/mL) and GS loaded CuS NPs (80 µg/mL; 40 µg/mL). All the treated plates were incubated at 37oC for 24 h and the zone of inhibition (in mm) was measured.

Results and Discussion

Antimicrobial resistance (AMR) is emerging as a global public health threat. With the tapered pipeline of antibiotic discovery, research has now been focussed on alternatives of antimicrobials. In recent times, nanotechnology has gained momentum in diverse fields such as antimicrobial and chemotherapeutic agents, drug delivery systems, photothermal therapy, and biosensors [19]. Owing to its high specific surface area to volume ratio, and anti-bactericidal activity, the CuS NPs were widely studied as effective nanomaterials in the fields of water treatment, antimicrobial food packaging and various biomedical applications [20]. However, the biosynthesis of CuS NPs using fungal agents has not widely been employed, barring a few studies [21]. Moreover, this appears to be the first study of its kind in the biosynthesis of CuS NPs employing the biocontrol fungi, T. harzianum.

Mycosynthesis of CuS NPs

In this study, the extract of T. harzianum reduced the aqueous solution of 2 mM copper sulphate (at a ratio of 1:4) to CuS NPs, upon incubation at 25°C under constant stirring (180 rpm) for 36 h (Figure 1a). The biocontrol fungus, T. harzianum was earlier used for the extracellular biosynthesis of silver NPs, in order to control an agricultural fungal infection- the white mold [22]. The formation of light green colored precipitate at the bottom of the conical flask in our study (Figure 1a) indicated the biosynthesis of CuS NPs [23].

The biosynthesis of CuS NPs employing the fungal biomass could possibly be due to the extracellular reduction of the copper ions in the copper sulphate solution forming nucleation, followed by accumulation and stabilization of CuS NPs, depending on various factors such as concentration of copper sulphate solution, reaction time and temperature [21]. Even though different concentrations of copper sulphate solution (1 mM, 2 mM, 5 mM and 10 mM) were employed in this study for the biological synthesis of CuS NPs, 2 mM was found to be optimal, based on the antibacterial activity on MH agar plates (data not shown). Moreover, the optimum ratio of fungal extract to copper sulphate solution for inducing the green synthesis of CuS NPs in this study was observed to be 1:4 (data not shown). Further, while employing the mycosynthesis of CuS NPs at varying temperatures (25°C, 50°C, and 70°C), a reaction temperature of 25°C was observed to be optimal.

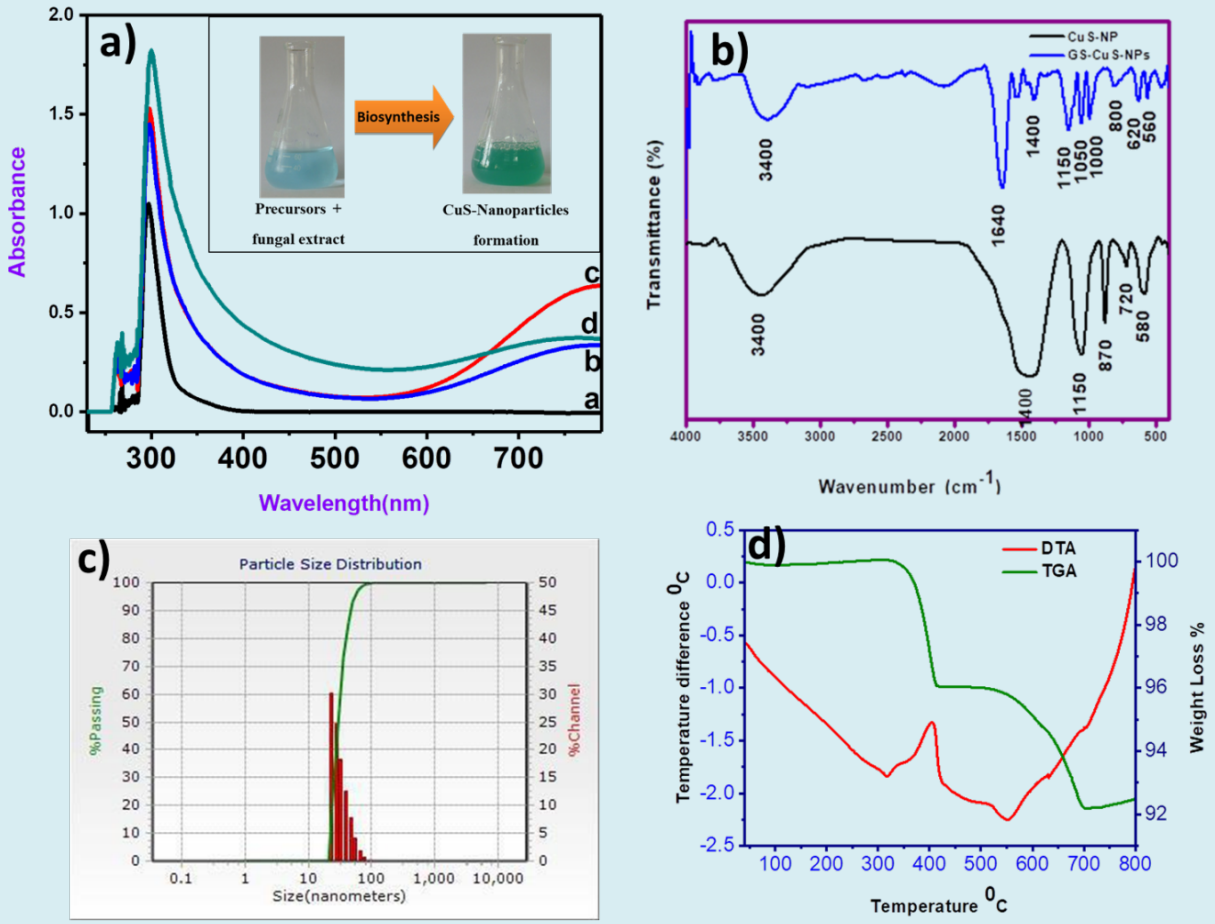

Figure 1: (a): UV-Vis spectra of CuS NPs prepared using 1mM (a), 2 mM(b), 5mM (c) and 10 mM (d) hydrated CuSO4 and T. harzianum; (b) FTIR spectra of CuS NPs and GS- laden CuS NPs; (c) Particle size distribution of biosynthesized CuS NPs; (d) TGA/DTA curve of biosynthesized CuS NPs.

Characterization of CuS NPs

Initially, the biosynthesized CuS NPs were characterized optically by using UV-Vis spectrophotometer for analyzing the surface plasmon resonance (SPR). The suspension of CuS NPs in nanopure water exhibited a maximum absorbance at 560 nm (Figure 1a).

The FTIR analysis of CuS NPs (Figure 1b) permits spectrometric observations within the range of 400-4000 cm-1. Moreover, the FTIR spectrum revealed characteristic bands corresponding to functional groups of biosynthesized CuS NPs. The spectrum observed between 500-600 cm-1 (Cu-S stretching mode) corresponds to the copper sulphide crystals, while at 1150 cm-1, 1400 cm-1, and 3400 cm-1 corresponds to the characteristic C-O stretching vibration, C-H stretching vibration and presence of OH functional groups, respectively (Figure 1b) [24,25].

Meanwhile, the size distribution and surface charge of biosynthesized CuS NPs was recorded by DLS. The average size of CuS NPs ranged between 40 to 90 nm, while the surface charge was observed to be -200 mV (Figure 1c). In this study, the mycosynthesised CuS NPs resulted in highly monodisperse nanoparticles with size ranging from 40 to 90 nm, as reported earlier [4].

In order to determine the thermal stability and thermal degradation of biosynthesized NPs under constant heating, thermogravimetric analysis (TGA) was carried out. The TGA data obtained in the present study revealed a thermal decomposition of CuS NPs started around 320°C supported

by the DTA with narrow endothermic dip at 320°C and the decomposition continued till 430°C. Moreover, a weight loss of 5% up to 430°C in TGA corresponded with a sharp intense exothermic peak in DTA observed at 430°C (Figure 1d). Further, a progressive thermal degradation of the biosynthesized CuS NPs were observed from 500°C that corresponded with a narrow endothermic peak (Figure 1d). In short, the results of TGA/ DTA indicated thermal decomposition and crystallization of the sample occurred simultaneously which is suggestive of thermal stability.

Further, the microscopic surface morphology and topographic information of CuS NPs was carried out by AFM analysis. In the present study, quantitative measurement of surface features such as two- and three- dimensional AFM topological images of CuS NPs were assessed (Figure 2a; 2b). It was estimated that the roughness average (Ra) and root mean square roughness (Rq) for the mycosynthesised CuS NPs were found to be 0.57 nm and 0.79 nm. Besides, the present study illustrated the presence of comparatively lesser dents and irregularities in the surface morphology of CuS NPs (Figure 2a; 2b), which is in contradiction with the earlier report [26], with higher Ra and Rq values.

The morphology and microstructure of the biosynthesized CuS NPs were visualized using SEM. The SEM imaging of CuS NPs, in this study, revealed rod to spherical shape (Figure 2c). The results of elemental analysis carried out by energy dispersive x-ray (EDX) indicated the presence of copper and sulfur (Figure 2d). The additional peaks visualized in the EDX spectra (Figure 2d) represent stabilizing agents that originated from the fungal extract [27].

The PXRD pattern of CuS NPs shown as Figure 3a exhibited planes at (022), (023) and (130) indexed to orthogonal structure (JCPDS Card No. 65-7111) [28,29].

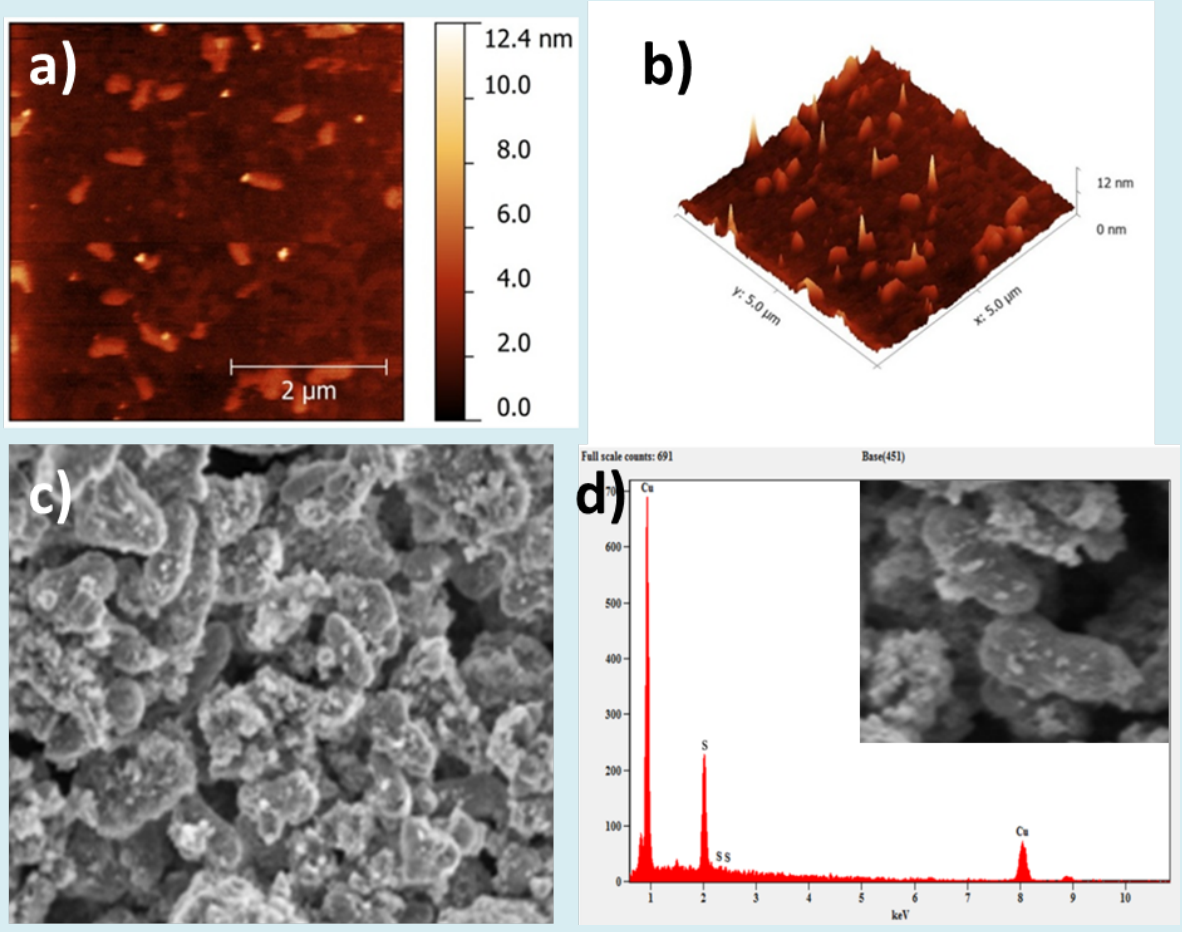

Figure 2: Surface topology and electron microscopic imaging of biosynthesized CuS NPs.
AFM imaging (a; b) of CuS NPs; SEM imaging (c) of CuS NPs; Elemental analysis (d) of biosynthesized CuS NPs.

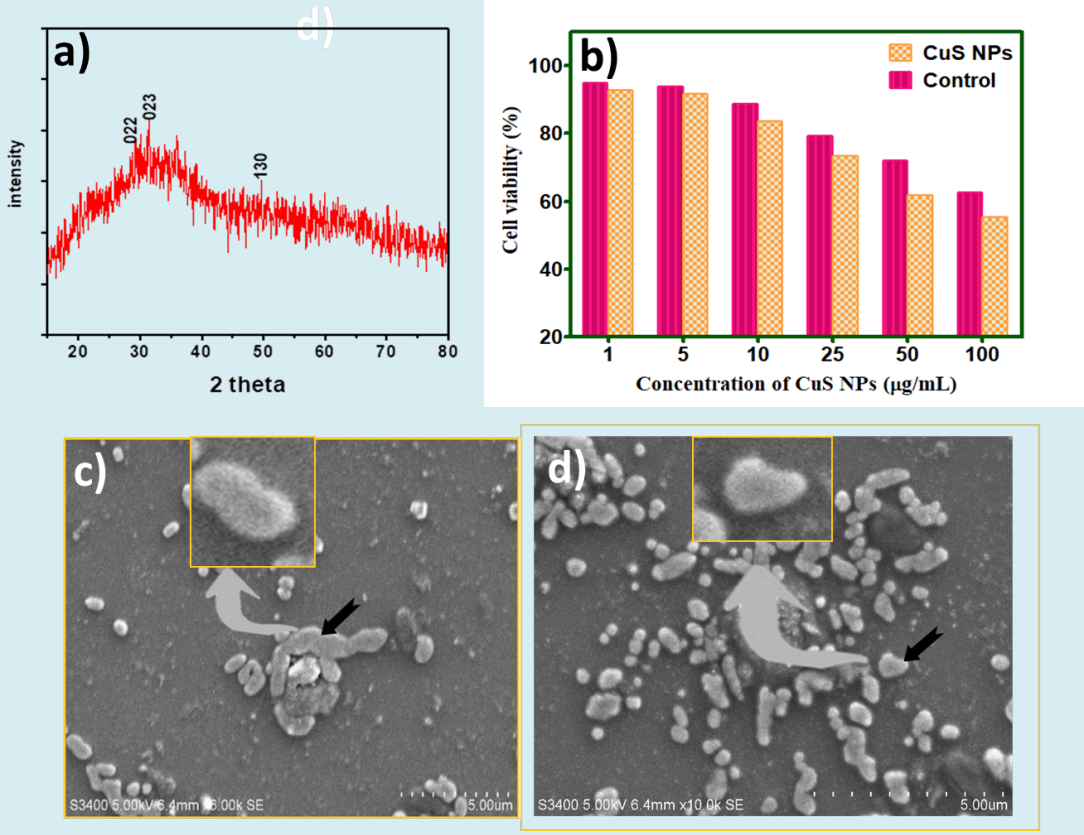

Figure 3: XRD pattern (a) of CuS NPs; MDA MB- 231 cell line- based viability assay (b) of CuS-NPs; SEM micrograph of CuS NPs untreated (c) and treated (d) B. subtilis, respectively

In Vitro Cytotoxicity Assay

The mycosynthesised CuS NPs were subjected to in vitro MTT cell line- based cytotoxicity assay as an indicator of cell viability, and proliferation [16,30]. In the present study, breast epithelial MDA MB- 231 cell line was employed to estimate the half- maximal inhibitory concentration (IC50) of the CuS NPs. The degree of cell viability decreased progressively with the increasing concentrations of mycosynthesised CuS NPs (Figure 3b). Further, the IC50 value of CuS NPs determined in this study was found to be 165 µg/mL. The results of this study indicate that the mycosynthesised CuS NPs were relatively non- toxic to the epithelial cell lines tested, as reported in earlier studies [31,32].

SEM Imaging of CuS Treated Bacteria

The fixed SEM- based visualization of B. subtilis (taken as a representative bacterial strain) treated with CuS NPs was carried out to observe the morphological changes, along with untreated bacterial control (Figure 4a; 4b).

In this study, the SEM imaging revealed that the CuS NPs did not penetrate the bacterial cells , which could be due to the comparatively bigger size of CuS NPs (40 to 90 nm) than the pores in the cell wall of Gram- positive bacteria (4-16nm) [33].

GS- Laden CuS NPs

In order to enhance the activity of biosynthesized CuS NPs, a broad- spectrum aminoglycoside antibiotic (GS) was used in this study. In general, GS inhibits the bacterial protein synthesis by binding to 30S ribosomal subunit and exerts bactericidal action [34]. The antibiotic GS was conjugated to the already synthesized CuS NPs [5] resulting in the formation of light greenish colored powder, indicating the entrapment of GS onto CuS NPs.

The GS- laden CuS NPs thus synthesized were characterized by FTIR spectroscopy (Figure 1b). On analyzing, the FTIR spectrum of GS- laden CuS NPs indicated a short peak at 1400 cm-1 due to -NH2 group, while the peaks

observed at 1050 cm-1 and 1150 cm-1 in the GS- laden CuS NPs corresponds to C-O stretching vibration. Moreover, the vibrations noticed at 560 cm-1 could be due to the presence of metal sulphide, whereas at 3400 cm-1 corresponds to O-H stretching. Besides, the FTIR spectra observed at 1640 cm-1 and 1530 cm-1 corresponds to the -NH groups of Gentamicin (Figure 1b) [35].

The application of CuS NPs as nano-based carriers were assessed by estimating the drug loading as well as entrapment efficiency. In the present study, the drug loading capacity and entrapment efficiency of the mycosynthesised CuS NPs were recorded as 39% and 61%, respectively. The findings of our study indicated that the mycosynthesised CuS NPs act as better vehicles for drug loading and entrapment towards GS than the earlier study which reported the loading of GS onto calcium carbonate NPs, wherein drug loading and entrapment efficiency was found to be 25.30% and 38.60%, respectively [36].

In Vitro Haemolytic Assay

The erythrocyte- mediated haemolytic assay of GS-loaded CuS NPs was determined to assess the initial toxicity. The erythrocyte is often employed as a model of host cell membrane to estimate the haemolytic activity as a tool for the rapid assessment of initial toxicity of antimicrobial agents. We employed chicken erythrocytes for determining the in vitro toxicity of GS- laden CuS NPs (100 µg/mL). A minimal haemolysis (5.05%) observed for the GS- laden CuS NPs in this assay indicated toxicity profile [37].

In Vitro Antibacterial Activity

An agar well diffusion method was employed to ensure the antibacterial activity of GS-laden CuS NPs in comparison with GS alone and CuS NPs against Gram negative as well as Gram positive bacterial pathogens.

From the Table 1, it was observed that the GS- laden CuS NPs (80 µg/mL) inhibited the growth of bacterial strains tested better than the free GS and CuS NPs estimated from the zone of inhibition. It is interesting to note that the loaded of GS with the CuS NPs enhanced its antibacterial activity. The pronounced in vitro antibacterial activity of GS- laden CuS NPs (80 µg/mL) than the GS- laden CuS NPs (40 µg/mL) might be due to the concentration- dependent characteristic of aminoglycoside class of antibiotics [5,38].

Candidate molecules	*E. coli*	*S.* Typhi	*K. pneumoniae*	*S. aureus*	*B. subtilis*
GS(30 µg/mL)	21±1	30±1	22±1	31±1	26±1
CuS NPs(0 µg/mL)	13±1	15±1	15±1	16±1	14±1
GS- laden CuS NPs(80 µg/mL)	25±1	27±1	27±1	33±1	29±1
GS- laden CuS NPs(40 µg/mL)	19±1	21±1	20±1	25±1	22±1

Table 1: In vitro antibacterial efficacy (measured in zone of inhibition, mm) of mycosynthesised CuS NPs, GS and GS- laden CuS NPs.

Conclusion

The CuS NPs were synthesized and characterized employing the fungal cell mass of biocontrol pest, T. harzianum. Later, gentamicin was loaded onto the mycosynthesised CuS NPs in order to assess the enhancement in its antibacterial activity. We observed a synergistic antibacterial efficacy of GS- laden CuS NPs against the pathogens tested. In short, the GS- laden CuS NPs were found to be effective candidates to combat pathogenic microorganisms. Moreover, the green synthesized CuS NPs as well as GS- laden CuS NPs in this study were found to be non- toxic towards the tested epithelial cell line. This study highlights an eco-friendly synthesis of semiconductor nanomaterials as potential drug carriers and opens the feasibility of biocompatible materials for drug loading in the field of nanomedicine.

References

1. Dorati R, DeTrizio A, Spalla M, Migliavacca R, Pagani L, et al. (2018) Gentamicin Sulfate PEG-PLGA / PLGA-H Nanoparticles : Screening Design and Antimicrobial Effect Evaluation toward Clinic Bacterial Isolates. Nanomaterials (Basel) 8(1): 37.

2. Chen C, Hsu C, Lai S, Syu W, Wang T, et al. (2014a) Metal Nanobullets for Multidrug Resistant Bacteria and Biofilms. Adv Drug Deliv Rev 78: 88-104.

3. Abishad P, Niveditha P, Unni V, Vergis J, Kurkure NV, et al. (2021) In Silico Molecular Docking and in Vitro Antimicrobial Efficacy of Phytochemicals Against Multi-Drug-Resistant Enteroaggregative Escherichia Coli and Non-Typhoidal Salmonella spp. Gut Pathog 13: 1-11.

4. Luthra S, Rominski A, Sander P (2018) The Role of Antibiotic-Target-Modifying and Antibiotic-Modifying Enzymes in Mycobacterium abscessus Drug Resistance. Front Microbiol 9: 1-13.

5. Imbuluzqueta E, Gamazo C, Lana H, Campanero MA, Salas D, et al. (2013) Hydrophobic Gentamicin-Loaded Nanoparticles are Effective Against Brucella Melitensis Infection in Mice. Antimicrob Agents Chemother 57(7): 3326-3333.

6. Wang L, Hu C, Shao L (2017) The Antimicrobial Activity of Nanoparticles: Present Situation and Prospects for the Future. Int J Nanomedicine 12: 1227-1249.

7. Goel S, Chen F, Cai W (2014) Synthesis and Biomedical Applications of Copper Sulfide Nanoparticles: from Sensors to Theranostics. Small 10(4): 631-645.

8. Byrappa K, Adschiri T (2007) Hydrothermal Technology for Nanotechnology. 53(2): 117-166.

9. Lellala K, Namratha K, Byrappa K (2016) Ultrasonication Assisted Mild Solvothermal Synthesis and Morphology Study of Few-Layered Graphene by Colloidal Suspensions of Pristine Graphene Oxide. Microporous and Mesoporous Materials 226: 522-529.

10. Srinath BS, Namratha K, Byrappa K (2017) Eco-Friendly Synthesis of Gold Nanoparticles by Gold Mine Bacteria Brevibacillus Formosus and their Antibacterial and Biocompatible Studies. IOSR Journal of Pharmacy 7(8): 53-60.

11. Mandal D, Bolander ME, Mukhopadhyay D, Sarkar G, Mukherjee P (2006) The Use of Microorganisms for the Formation of Metal Nanoparticles and Their Application. Appl Microbiol Biotechnol 69(5): 485-492.

12. El-Moslamy SH, Elkady MF, Rezk AH, Abdel-Fattah YR (2017) Applying Taguchi Design and Large-Scale Strategy for Mycosynthesis of Nano-Silver from Endophytic Trichoderma Harzianum SYA.F4 and its Application Against Phytopathogens. Sci Rep 7: 1-22.

13. Yadav A, Kon K, Kratosova G, Duran N, Ingle AP, et al. (2015) Fungi as an Efficient Mycosystem for the Synthesis of Metal Nanoparticles: Progress and Key Aspects of Research. Biotechnol Lett 37(11): 2099-2120.

14. Yoshizawa S, Fourmy D, Puglisi JD (1998) Structural Origins of Gentamicin Antibiotic Action. EMBO J 17: 6437-6448.

15. Díez-martínez R, García-fernández E, Manzano M, Martínez A, Domenech M, et al. (2016) Auranofin-Loaded Nanoparticles as a New Therapeutic Tool to Fight Streptococcal Infections. Sci Rep 6: 1-12.

16. Mosmann T (1983) Rapid Colorimetric Assay for Cellular Growth and Survival: Application to Proliferation and Cytotoxicity Assays. J Immunol Methods 65(1-2): 55-63.

17. Chen C, Hsu C, Lai S, Syu W, Wang T, et al. (2014b) Metal Nanobullets For Multidrug Resistant Bacteria And Biofilms. Adv Drug Deliv Rev 78: 88-104.

18. Babu EP, Subastri A, Suyavaran A, Premkumar K, Sujatha V, et al. (2017) Size Dependent Uptake and Hemolytic Effect of Zinc Oxide Nanoparticles on Erythrocytes and Biomedical Potential of ZnO-Ferulic acid Conjugates. Sci Rep 7: 1-12.

19. Canaparo R, Foglietta F, Giuntini F, Pepa C, Dosio F, et al. (2019) Recent Developments in Antibacterial Therapy : and Therapeutic Nanoparticles. Molecules 24(10):1-15.

20. Anvar AA, Ahari H, Ataee M (2021) Antimicrobial Properties of Food Nanopackaging: A New Focus on Foodborne Pathogens. Front Microbiol 12.

21. Mukherjee P, Ahmad A, Mandal D, Senapati S, Sainkar SR, et al. (2001) Fungus-Mediated Synthesis of Silver Nanoparticles and Their Immobilization in the Mycelial Matrix: A Novel Biological Approach to Nanoparticle Synthesis. Nano Lett 1(10): 515-519.

22. Guilger M, Pasquoto-Stigliani T, Bilesky-Jose N, Grillo R, Abhilash P, et al. (2017) Biogenic Silver Nanoparticles Based on Trichoderma Harzianum: Synthesis, Characterization, Toxicity Evaluation and Biological Activity. Sci Rep 7: 1-13.

23. Solanki JN, Sengupta R, Murthy ZVP (2010) Synthesis of Copper Sulphide and Copper Nanoparticles with Microemulsion Method. Solid State Science 12(9): 1560-1566.

24. Saranya M, Santhosh C, Ramachandran R, Nirmala Grace A (2014) Growth of CuS Nanostructures by Hydrothermal Route and its Optical Properties. J Nanotechnol 1-8.

25. Wang Y, Jiang F, Chen J, Sun X, Xian T, et al. (2020) In Situ Construction of CNT/CuS Hybrids and Their Application in Photodegradation for Removing Organic Dyes. Nanomaterials 10(1): 178.

26. Ajibade P, Botha N (2017) Synthesis, Optical and Structural Properties of Copper Sulfide Nanocrystals from Single Molecule Precursors. Nanomaterials 7: 32.

27. Ottoni CA, Simões MF, Fernandes S, Gomes dos Santos J, Sabino da Silva E, et al. (2017) Screening of Filamentous Fungi for Antimicrobial Silver Nanoparticles Synthesis.

AMB Express 7(1): 31.

28. Qi J, Wen J, Wang Q, Jin X, Zhou X (2020) Preparation and Photocatalytic Properties of Hexagonal and Orthogonal Cus Micro-Nanoparticles by an Oil-Water Interface Method. Mater Chem Phys 255: 123629.

29. Zhou NQ, Tian LJ, Wang YC, Li DB, Li PP, et al. (2016) Extracellular Biosynthesis of Copper Sulfide Nanoparticles by Shewanella Oneidensis MR-1 as a Photothermal Agent. Enzyme Microb Technol 95: 230-235.

30. Van Tonder A, Joubert AM, Cromarty AD (2015) Limitations of the 3-(4,5-Dimethylthiazol-2-Yl)-2,5-Diphenyl-2H-Tetrazolium Bromide (MTT) Assay when Compared to Three Commonly Used Cell Enumeration Assays. BMC Res Notes 8(47): 1-10.

31. Feng W, Nie W, Cheng Y, Zhou X, Chen L, et al. (2015) In Vitro and in Vivo Toxicity Studies of Copper Sulfide Nanoplates for Potential Photothermal Applications. Nanomedicine: Nanotechnology Biology and Medicine 11(4): 901-912.

32. Wang C, Kim YJ, Singh P, Mathiyalagan R, Jin Y, et al. (2016) Green Synthesis of Silver Nanoparticles by Bacillus Methylotrophicus, and their Antimicrobial Activity. Artificial Cells, Nanomedicine Biotechnology 44(4): 1127-1132.

33. Pajerski W, Ochonska D, Brzychczy-Wloch M, Indyka P, Jarosz M, et al. (2019) Attachment Efficiency of Gold Nanoparticles by Gram-Positive and Gram-Negative Bacterial Strains Governed by Surface Charges. J Nanoparticle Res 21: 186.

34. Papich MG (2016) Gentamicin Sulfate. Saunders Handb Vet Drugs pp: 353-355.

35. Dizaj SM, Barzegar-jalali M, Zarrintan MH, Adibkia K, Lotfipour F (2015) Calcium Carbonate Nanoparticles as Cancer Drug Delivery System. Expert Opinion on Drug Delivery 12(10): 1649-1660.

36. Maleki Dizaj S, Lotfipour F, Barzegar-Jalali M, Zarrintan M, Adibkia K (2016) Physicochemical Characterization and Antimicrobial Evaluation of Gentamicin-Loaded Caco3nanoparticles Prepared Via Microemulsion Method. J Drug Deliv Sci Technol 35: 16-23.

37. Zare M, Namratha K, Thakur MS, Yallappa S, Byrappa K (2018) Comprehensive Biological Assessment and Photocatalytic Activity of Surfactant Assisted Solvothermal Synthesis of Zno Nanogranules. Mater Chem Phys 215: 148-156.

38. Kotian SY, Abishad PM, Byrappa K, Rai KML (2019) Potassium Iodate (KIO 3) as a Novel Reagent for the Synthesis of Isoxazolines: Evaluation of Antimicrobial Activity of the Products. J Chem Sci 131(46): 1-6.